

Title	Structural change in p-type porous silicon by thermal annealing
Author(s)	Ogata, YH; Yoshimi, N; Yasuda, R; Tsuboi, T; Sakka, T; Otsuki, A
Citation	JOURNAL OF APPLIED PHYSICS (2001), 90(12): 6487-6492
Issue Date	2001-12-15
URL	http://hdl.handle.net/2433/50429
Right	Copyright 2001 American Institute of Physics. This article may be downloaded for personal use only. Any other use requires prior permission of the author and the American Institute of Physics.
Type	Journal Article
Textversion	publisher

Structural change in *p*-type porous silicon by thermal annealing

Yukio H. Ogata,^{a)} Naoki Yoshimi, Ryo Yasuda, Takashi Tsuboi, Tetsuo Sakka, and Akira Otsuki

Institute of Advanced Energy, Kyoto University, Uji, Kyoto 611-0011, Japan

(Received 17 April 2001; accepted for publication 13 September 2001)

The morphological change of *p*-type porous silicon during annealing has been investigated. The x-ray diffraction (XRD) pattern was composed of a sharp Bragg reflection peak and a diffuse scattering. The diffuse scattering is not related to the presence of the amorphous phase. The shape of the XRD pattern started to change at an annealing temperature as low as 400 °C, and the 2θ angle of the sharp peak varied at a temperature as low as 350 °C. These changes at low temperatures seem to be closely related to the desorption of hydrogen and the resultant change of the dangling bond density in porous silicon. The molecular orbital calculations also support the participation of dangling bonds in the structural reorganization in the surface region. © 2001 American Institute of Physics. [DOI: 10.1063/1.1416862]

I. INTRODUCTION

Porous silicon (PS) is usually prepared by anodizing a Si wafer in hydrofluoric (HF) solution. A variety of morphology can be produced depending upon the type of silicon substrate and the preparation conditions.^{1–3} Among these, the morphology of PS prepared from nondegenerate *p*-type Si wafers (*p*-PS) in HF solution indicates a labyrinthine structure with nanometer-sized pores,⁴ and a complete understanding of the structure has not been attained yet. The image that is observed by a transmission electron microscope (TEM) sometimes implies the presence of amorphous phase in PS. In early works, the presence of an amorphous phase⁵ and polycrystal⁶ in the layer had been proposed. However, subsequent studies using x-ray multichannel diffractometry revealed the monocrystallinity resulting from selective dissolution at the bottom of pores leaving the original crystal structure.^{7–10} TEM observations show us an amorphous-like image in porous silicon prepared from a nondegenerate *p*-type silicon wafer.^{11,12} On the other hand, x-ray diffraction (XRD) measurements present a noticeable feature related to the crystallinity. Each diffraction peak consists of a sharp peak and broad diffraction around the peak.^{13–16} The latter becomes significant as the resistivity of the substrate increases. It has been considered that the broad scattering is attributed to microcrystallites and the strained structures,¹³ or randomly distributed pores.¹⁴

If a specimen is observed using XRD and TEM, the results should not give contradictory information. However, the structure of the TEM image has not been well understood in connection with the XRD pattern. We occasionally find reports describing the amorphous phase in PS. This is probably because the origin of the amorphous-like image in the TEM observation has not yet been understood. We have found that the shape of the diffuse x-ray diffraction changes when porous silicon is annealed, and the behavior can provide a clue to understanding the complicated structure.

The present study investigates XRD of PS prepared from a *p*-type Si wafer with relatively high resistivity and also the TEM image. The structural change by sample annealing is investigated. We then discuss the crystallinity in PS. We also present the change and investigate the cause focusing on the reorganization of bonding states and structure that are brought by thermal annealing.

II. EXPERIMENT

PS was prepared from a boron-doped *p*-type (100) Si wafer (10–20 Ω cm) in 48 wt. % HF solution at an anodic current density of 10 mA cm⁻² for 7 h. The PS layer was removed from the substrate by applying a high current density greater than 1 A cm⁻². The ohmic contact was made by Al deposition at the back side and subsequent annealing, except for the samples for infrared spectroscopy. The porosity was about 70%. The PS was dried by blowing Ar gas for 5 min immediately after preparation, followed by storing in a desiccator containing silica gel for longer than 12 h. Thermal annealing was performed at different temperatures ranging from 200 to 800 °C in a vacuum furnace, the base pressure of which was 8×10^{-6} Pa. The PS sample was kept at a desired temperature for 30 min. The specimens were fully pulverized in an agate mortar.

The samples were fixed with paraffin liquid on a reflectionless glass plate and analyzed using an x-ray diffractometer (Rigaku, RAD) with Cu $K\alpha$ under the conditions of 40 kV, 25 mA, and using a stepping width of 0.05°. The diffraction was compared with those of crystalline silicon *c*-Si, and amorphous silicon *a*-Si, which was prepared from sputtering and did not contain hydrogen. The thermal behavior was investigated with differential thermal analysis (DTA) (Rigaku, TG8110), where the temperature was scanned at 10 °C min⁻¹. Transmission Fourier transform infrared (FTIR) spectra were measured using a Nicolet Avatar 360 spectrometer. We used the mixture of the pulverized PS and KBr powder as the sample, of which the ratio was 1:100. The data obtained by 64 scans were collected and the resolution was 1

^{a)} Author to whom correspondence should be addressed; electronic mail: y-ogata@iae.kyoto-u.ac.jp

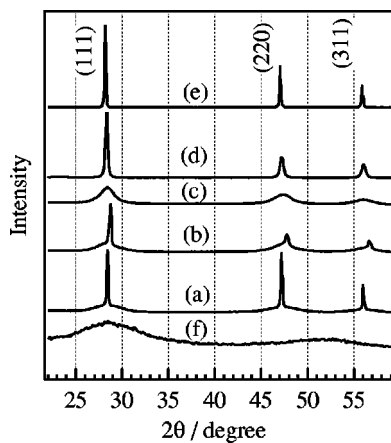


FIG. 1. XRD profiles of *p*-PS annealed at various temperatures: (a) as prepared, (b) 350 °C, (c) 450 °C, and (d) 700 °C. The samples were kept at the temperatures for 30 min. The profiles of (e) ground silicon wafer *c*-Si and (f) α -Si prepared by sputtering are shown as reference.

cm^{-1} . The electron spin resonance (ESR) spectroscopy was performed to measure the dangling bond density using an ESR spectrometer (JEOL, JES-TE200).

The morphology of *p*-PS was observed by TEM (JEOL, JEM4000EX). The PS layer was scraped off from the substrate, then ground in a mortar. Thus prepared small flakes were fixed on a supporting grid as specimens for observation. It is known that the sample preparation must be very careful because it causes the sample to be amorphous during the preparation, especially during thinning by ion milling.^{17,18} This was true in the present samples, and hence the specimen was prepared from a flake without mechanical and physical thinning.

III. RESULTS

Figure 1 shows XRD profiles of *p*-PS treated at different temperatures. Each diffraction line is composed of two characteristic sharp and diffuse patterns. The shape of a sharp peak is superimposed by a broad pattern as previously observed.^{13–16} The broad pattern became prominent as HF concentration for the preparation decreased: the sharp Bragg peak was hard to observe in the *p*-PS sample prepared in 15 wt. % HF solution. In contrast, *p*⁺-PS prepared from a *p*⁺-type silicon wafer (0.01–0.02 Ωcm) showed the dominance of the sharp diffraction. The shape changed with heat treatment.

The sharp peak disappeared after annealing at a temperature over 450 °C, giving a relatively broad peak. When the temperature was increased to 700 °C, the sharpness recovered. At temperatures lower than 450 °C, the peak position of the sharp peak shifted toward the high angle direction when the sample was annealed (Fig. 2). The 2θ angle for the sharp peak of the as-prepared sample was a little smaller than that of crystalline Si prepared from a Si wafer. The angle became large as the temperature was increased. The sharp peak disappeared at temperatures between 400 and 450 °C. Meanwhile, it seems that there was no change in the peak position of the diffuse scattering with varying annealing temperatures, and the sharpening of the diffuse scattering after the disap-

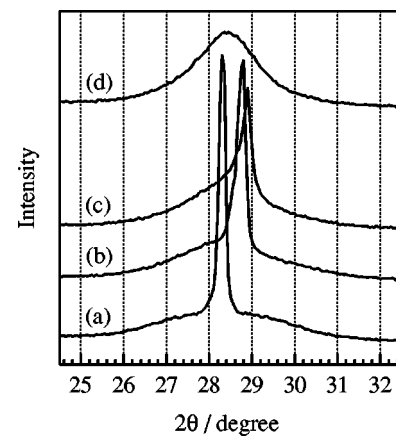


FIG. 2. Peak shift of (111) diffraction for the samples after annealing at: (a) as prepared, (b) 350 °C, (c) 400 °C, and (d) 450 °C.

pearance of the sharp diffraction occurred without the peak shift. The variation of the relative lattice spacing, which is estimated from the (111) diffraction using the Bragg law with annealing temperature, is shown in Fig. 3. It should be noted that the values at temperatures higher than 450 °C were taken from the peaks that were developed from the diffuse scattering.

Figure 4 shows the variation of the FTIR spectrum of PS after annealing at different temperatures. Si–H species except for the monohydrides are almost desorbed by 350 °C,¹⁹ and all the hydrogen species were removed by 500 °C. The as-prepared sample already shows an absorption peak around 1100 cm^{-1} , which can be assigned to Si–O–Si stretching. It is true that porous silicon is oxidized in air to a certain degree. However, the rate is not very fast because of the stabilization effects due to the hydrogen termination. For example, a sample kept in dry air at 60 °C is oxidized but not severely. This is proved by the FTIR spectrum as shown in our previous work (Fig. 1 in Ref. 20). Therefore, at room temperature it is hard to imagine that our samples were completely oxidized. This is further confirmed by Fig. 1 in Ref. 19, Fig. 1 in Ref. 21, and others. The absorption did not develop after annealing and we did not observe appreciable absorption due to the backbond oxidation in the wave num-

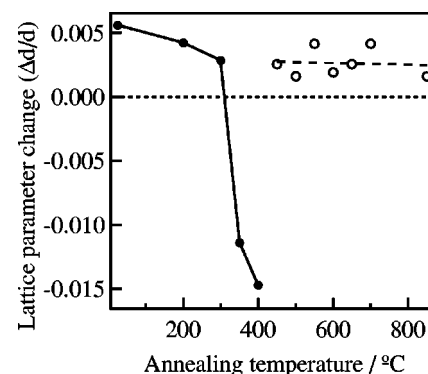


FIG. 3. Lattice spacing change calculated from the peak angle of (111) diffraction with varying annealing temperature. Solid circles show the results from the originally existed diffraction, and open circles are from the diffraction developed from the diffuse scattering.

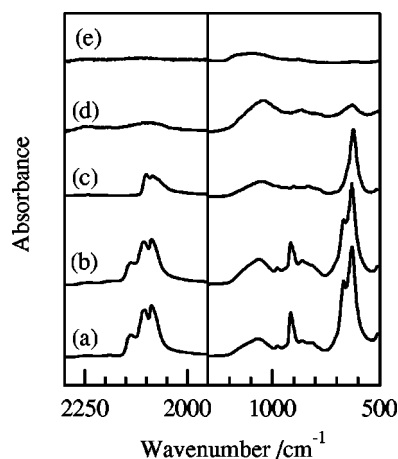


FIG. 4. FTIR spectra of annealed PS at: (a) as prepared, (b) 200 °C, (c) 350 °C, (d) 450 °C, and (e) 700 °C.

bers from 2160 to 2250 cm^{-1} ,²⁰ therefore we can conclude that no appreciable oxidation of PS proceeded on the sample. The samples used in the present work were prepared as we did in the previous works.^{19–21} The only difference in the FTIR sample preparation between the present work and the previous studies was the dilution of the sample volume by a KBr powder. (The use of a KBr powder is quite common in FTIR investigation.) Heat treatment at high temperatures causes separation of the porous layer from the substrate in the form of flakes. Therefore, we used the above-mentioned powder instead of a porous layer on the substrate. The presence of KBr caused the appearance of absorption at 1100 cm^{-1} even by using carefully dried KBr. It seems, however, that the mechanism which causes the 1100 cm^{-1} peak does not substantially affect the oxidation of porous silicon. The Si–O–Si vibration has a large absorption coefficient. The intensity in Fig. 4 indicates that the oxidation was not severe if at all. Thus, the peak is not from the oxidation of porous silicon. Even if there were a slight oxidation, it would not affect our discussion to a large extent. Furthermore, a complete oxidation to the extent of being amorphous should indicate a diffuse pattern peaking at around $2\theta = 20^\circ$ (Cu $K\alpha$); however, there is no indication of this scattering peak in the diffraction pattern (Fig. 1). The desorption causes the formation of dangling bonds in PS. The density was measured by ESR. The variation with temperature is shown in Fig. 5. The

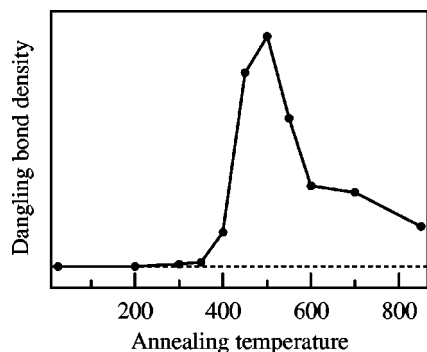


FIG. 5. Dangling bond density measured by ESR as a function of annealing temperature.

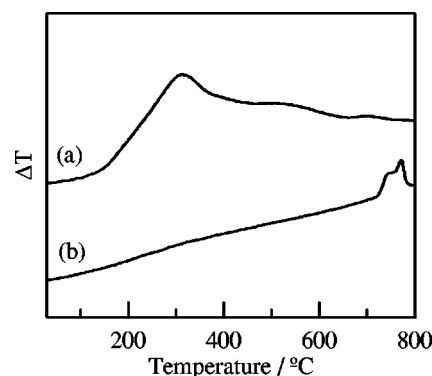


FIG. 6. Differential thermal analysis of: (a) PS and (b) *a*-Si. *a*-Si was prepared by sputtering and hence did not contain hydrogen. Scan rate was 10 °C min^{-1} .

density of dangling bonds started increasing at 350 °C, reached a maximum at 500 °C, and then decreased. The behavior is similar to that reported for the PS prepared from n^+ -type Si.²² The coincidence between temperatures exhibiting the maximum dangling bonds and the minimum lattice spacing has been observed in the n^+ -PS. However, we could not confirm the coincidence since the sharp peak disappeared at temperatures between 400 and 450 °C. The DTA results also showed the desorption of hydrogen related species [Fig. 6(a)]. The desorption temperature is closely related to the results of the FTIR shown in Fig. 4.

The morphological observation was conducted using TEM (Fig. 7). No characteristic morphological structures such as pores were observed in *p*-PS. Lattice patterns could be observed only in a small part of the high-resolution TEM image and the electron diffraction (ED) showed a halo pattern with faint spots and rings. Heat treatment at temperatures higher than 400 °C developed the lattice patterns. When we observed an as-prepared p^+ -PS sample, we could find a branched columnar structure of several nanometers in the PS as reported⁴ and the dominance of lattice patterns in the high-resolution image.

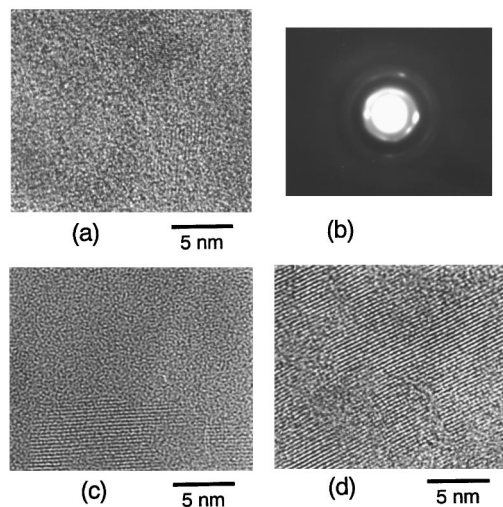


FIG. 7. High-resolution TEM images of *p*-PS prepared from 48% HF solution. Annealing temperatures are: (a) as prepared and its ED (b), (c) 400 °C, and (d) 800 °C.

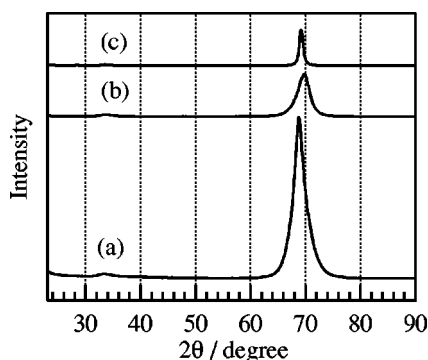


FIG. 8. XRD profiles of free-standing PS samples: (a) as prepared, annealed at (b) 400 °C, and at (c) 600 °C. The sample was set on an antireflection glass plate.

IV. DISCUSSION

A. Crystallinity of porous silicon

The properties of a specimen measured with different techniques must not give contradictory results. We used the same sample for the XRD and TEM measurements. It is necessary to explain the relation between the characteristic features obtained by the two techniques, that is, diffuse scattering in the XRD patterns, and the presence of disordered structures in the TEM images and the subsequent halo in the ED pattern. X-ray multidiffraction has revealed that PS has a monocrystalline character and the lattice expands slightly in comparison with bulk silicon.^{7–10} The dual structure of the XRD pattern consisting of a sharp peak and diffuse scattering has been observed.^{13–16} Some researchers consider that the diffuse structure is attributed to the minute size and the lattice distortion of crystallites introduced during porous layer formation.¹³ Meanwhile, Bensaid *et al.*¹⁴ considered that the diffuse scattering was caused by the presence of randomly distributed pores with nanometer size in PS.

Assuming that microcrystallites and strain are responsible for the diffuse diffraction, the size and the strain for PS prepared in 48 wt.% HF in the present experiments can be estimated to be about 3 nm and 0.025, respectively, from the analysis of the XRD diffraction using the Hall–Williamson plot.²³ The size corresponds roughly to the size of islands of lattice patterns in the TEM image; that is 3–6 nm. However, there is no answer of which part in the TEM image causes the sharp Bragg reflection in the XRD pattern if the islands are assigned to microcrystallites causing the diffuse scattering. We also conducted the XRD measurements using a free-standing PS sample instead of the pulverized powder. Figure 8 shows the result. Only the diffraction from the (400) face was observed, in which we used the usual θ – 2θ method. This is because the ratio of incident angle and 2θ satisfying the Bragg condition is held at 1:2 only at the (400) face. The results suggest that PS is uniquely oriented even after porous layer formation as reported previously¹ and after subsequent annealing. If randomly distributed crystallites were formed, we would have observed some diffraction peaks other than that from the (400) face of free-standing PS. Furthermore, the microcrystallites and strain model cannot explain the dual structures in the XRD and TEM results.

On the other hand, the random pore model proposed by Bensaid *et al.*¹⁴ seems appropriate for explaining the dual structures. The sharp peak and the lattice pattern may be attributed to the original crystalline, and the diffuse scattering and the amorphous-like phase are to the random pores. The latter does not disturb the long-range order because dissolution proceeds selectively or the silicon substrate holds its original crystallinity. We tried to verify this random pore model. We considered that visible photoluminescent behavior should vary if thermal annealing would cause PS structure change from that producing the quantum effects to the inactive structure. The as-prepared sample showed the typical spectrum with the peak intensity at ~ 650 nm. Annealing at 300 °C decreased the intensity greatly, and no appreciable photoluminescence could be detected for the sample treated at 350 °C. The change takes place at too low temperatures to be attributed to the morphological change. It is more probable that the change is caused by the change in the state of hydrogen rather than the morphological change judging from the change of the FTIR spectrum shown in Fig. 4, where only the monohydrides remain after the treatment at 350 °C. It seems that hydrogen desorption influences the photoluminescent behavior more than the morphological changes do, if any. As for the random micropores, we do not have the negative results, nor do we have the supporting results, at present.

The disordered structure in the TEM image reminds us of the presence of the amorphous phase. Although many researchers have reached a negative conclusion,^{7–10} some researchers still consider its presence. Here, we consider the possibility in *p*-PS again. Figure 1 shows the comparison of the XRD patterns among differently prepared silicon samples: *c*-Si, *p*-PS, and *a*-Si. The sharp peak of PS almost coincides with the diffraction from the crystalline phase that can be observed in *c*-Si. The feature of the broad peak was different from that of *a*-Si. A broad peak for *a*-Si extended between diffraction from (220) to (311) faces of *c*-Si, while the broad peak was located exactly at each sharp peak in *p*-PS, where no enhancement of diffraction between (200) and (311) faces could be observed. Pulverized porous silicon was utilized for the XRD measurements, while the XRD of the free-standing film was also measured (Fig. 8). Monocrystalline silicon (100) shows only a diffraction peak from the (400) face, and the free-standing PS exhibited one peak as well. If the amorphous phase existed with such an amount giving the disordered region in the TEM image (Fig. 7) or the diffuse scattering in the XRD pattern (Fig. 1), the phase would be predominant. Consequently, we would not observe an appreciable diffraction at an angle of the (400) face in the result of *p*-PS. DTA measurements also revealed different behaviors between *p*-PS and *a*-Si. The *a*-Si was subjected to transition from amorphous to crystalline at a temperature of about 720 °C [Fig. 6(b)]; however, such a transition was not detected in *p*-PS. The amorphous–crystalline transition temperature has been reported to be 665 °C for hydrogen containing amorphous silicon prepared by thermal decomposition of silane.²⁴ The XRD and DTA results support the absence of the amorphous phase in *p*-PS. Our previous nuclear magnetic resonance measurements²¹ also support

this, where the spectrum of *p*-PS was much different from that of *a*-Si.

B. Structural change of porous silicon with heat treatment

The XRD and DTA results suggest the absence of amorphous phase in *p*-PS, and other models so far have not been able to explain satisfactorily the dual structures observed in the XRD patterns and the TEM images. The structural change in *p*-PS with thermal annealing may give some information as to the dual structures. The change occurs at a temperature as low as 400 °C, as can be seen in the XRD and TEM image. The temperature is very low compared to the transition temperature from amorphous to crystalline, which can be seen in the DTA result of *a*-Si (Fig. 6). There is a significant increase in the area that exhibits lattice patterns in the TEM image, and sharpening of the diffuse scattering in the XRD pattern starts when annealing temperature increases further. The results again confirm the absence of the amorphous phase. The amorphous–crystalline transition takes place when the temperature is higher than 700 °C, but the transition could not be expected at 400 °C, although the transition temperature falls to some extent with increasing hydrogen content in PS;²⁴ on the other hand, the morphological change seems consecutive between these temperatures.

Figures 1 and 3 tell us that the diffuse part does not change its position after annealing at different temperatures, the sharp peak disappears by 450 °C, and the subsequent sharpening at the higher temperatures grows from the broad peak, of which the position does not shift with increasing annealing temperature. This is the case for *p*-PS. On the other hand, *p*⁺-PS behaved differently. The XRD peak was composed of a sharp peak accompanied by indistinct diffuse scattering although the diffuse scattering became appreciable when PS formation was performed in dilute HF solution. The disappearance of the peak was not observed. The peak shifted its position to a high angle at 400 °C. Around the temperature, the intensity decreased and the width became a bit large. After higher temperature treatment, the peak returned its position to the original value, and the intensity and the width recovered. The observations may imply the possibility that the sharp peak for *p*-PS after annealing would not disappear completely but would be concealed by the diffuse pattern. It is probable that the behavior is basically similar between *p*-PS and *p*⁺-PS. If so, the recovery of lattice spacing at high temperature annealing is expected. TEM observation of as-prepared *p*⁺-PS showed an image similar to that of *p*-PS obtained after high temperature annealing. These observations suggest that the structure of *p*-PS approaches an ideal single crystalline structure and the diffuse pattern in XRD and the amorphous-like image in TEM is closely related to each other.

Since desorption of hydrogen from the PS layer proceeds at 400 °C, it is expected that the change should be assisted by hydrogen desorption. Desorption of hydrogen species, especially SiH₃ and SiH₂, starts at temperatures of 260 °C or lower.¹⁹ The increase in the 2θ angle or the decrease in lattice spacing for the sharp peak in the XRD starts at temperatures as low as 350 °C (Fig. 3). The dangling bond density

TABLE I. Optimized geometric parameters for SiH_x.

Surface species	Model cluster	Si–Si spacing (Å)
≡SiH	(H ₃ Si) ₂ –HSi–SiH–(SiH ₃) ₂	2.386 (HSi–SiH)
	HSi–(SiH ₃) ₃	2.361
=SiH ₂	H ₃ Si–SiH ₂ –SiH ₃	2.356
–SiH ₃	H ₃ Si–SiH ₃	2.352
Si–Si (crystal)	—	2.352
≡Si•	(H ₃ Si) ₂ –•Si–SiH–(SiH ₃) ₂	2.378 (•Si–SiH)
	•Si–(SiH ₃) ₃	2.352
=SiH•	H ₃ Si–•SiH–SiH ₃	2.350
–•SiH ₂ •	•SiH ₂ –SiH ₃	2.347

measured by ESR also starts increasing at this temperature (Fig. 5). The temperature coincides with the temperature at which most dihydrides and trihydrides are removed from PS, as can be seen in Fig. 4. The desorption reorganizes the state of hydride and the dominant hydrogen species become monohydrides, especially (SiH)₂ dimers.¹⁹ Further desorption of hydrogen produces dangling bonds, since monohydrides cannot reorganize their structures without partial dangling bond formation, whereas reorganization with the formation of monohydride dimers is possible in the case of desorption from dihydrides or trihydrides. The effect of the presence of dangling bonds on the Si–Si bond length was estimated by molecular orbital calculations using the GAUSSIAN 94 program,²⁵ where the basis set of 6-31G* was used. The results are given in Table I. The introduction of dangling bonds makes the Si–Si bond length shorter. This corresponds to the decrease of lattice spacing with increasing annealing temperature as shown in Fig. 3. At temperatures higher than 500 °C, the FTIR spectra show no appreciable amount of hydrogen remaining in PS, and dangling bond density decreases because of the reorganization of Si atoms. The reorganization produces quite a well organized structure. The ideal (100) surface leaves some dangling bond density.²⁶ This is reflected in the sharpening of the diffraction peak and also the nonzero dangling bond density at high temperatures. There remain some questions for this model. For example, it is unclear whether such a surface change can dominate the bulk properties obtained by XRD, namely the peak shift, even though PS has a large surface area. However, this model can explain our experimental results and it is valuable to consider the mysterious dual structure further.

V. CONCLUSIONS

We investigated the possibility and the origin of the dual structure of XRD patterns and of the two types of morphology in TEM images for *p*-PS. The possible cause for the amorphous-like image and the diffuse diffraction in ED and XRD may be attributed to oxidation of PS, microcrystallites and strain,¹³ distortion of crystallites,¹⁷ or randomly distributed micropores.¹⁴ The clarification has yet to be attained. However, the present investigations including the comparison of other types of silicon and the structural changes by annealing revealed some important aspects for *p*-PS as follows:

- (1) There is no amorphous phase in *p*-PS.

- (2) The structural change starts at temperatures as low as 450 °C. There is no abrupt change in the TEM image by increasing temperature. The area indicating lattice patterns increases its ratio gradually. The dual structure of the XRD patterns disappears at this temperature, i.e., the disappearance of the sharp diffraction peak and the growth and sharpening of the diffuse part.
- (3) Diffuse scattering in the XRD and amorphous-like image in the TEM seem to be closely related to each other.
- (4) The formation of dangling bonds starts after the desorption of trihydrides and dihydrides. The presence makes it possible to reorganize the surface structure even at temperatures as low as 350 °C. The dangling bonds play an important role in the structural change and also at higher temperatures.

ACKNOWLEDGMENTS

The authors would like to thank Y.-I. Suzuki, C. Uye-mura Co., for the thermal analyses, and Professor R. E. Hummel, University of Florida, for useful discussion and improvement of the manuscript. The research was partly supported by a Grant-in-Aid from the Ministry of Education, Culture, Sports, Science and Technology, Japan.

¹R. L. Smith and S. D. Collins, *J. Appl. Phys.* **71**, R1 (1992).

²P. C. Searson, in *Advances in Electrochemical Science and Engineering*, edited by H. Gerischer and C. W. Tobias (VCH, Weinheim, 1995), Vol. 4, p. 67.

³A. G. Cullis, L. T. Canham, and D. J. Calcott, *J. Appl. Phys.* **82**, 909 (1997).

⁴M. I. J. Beale, J. D. Benjamin, M. J. Uren, N. G. Chew, and A. G. Cullis, *J. Cryst. Growth* **73**, 622 (1985).

⁵D. R. Turner, *J. Electrochem. Soc.* **105**, 402 (1958).

⁶Y. Arita and U. Sunohara, *J. Electrochem. Soc.* **124**, 285 (1977).

⁷K. Barla, R. Herino, G. Bomchil, J. C. Pfister, and J. Bruchel, *J. Cryst. Growth* **68**, 721 (1984).

⁸K. Barla, R. Herino, G. Bomchil, J. C. Pfister, and A. Freund, *J. Cryst. Growth* **68**, 727 (1984).

⁹I. M. Young, M. I. J. Beale, and J. D. Benjamin, *Appl. Phys. Lett.* **46**, 1133 (1985).

¹⁰H. Sugiyama and O. Nittono, *J. Cryst. Growth* **103**, 156 (1990).

¹¹Z. Yamani, O. Gurdal, A. Alql, and M. H. Nayfeh, *J. Appl. Phys.* **85**, 8050 (1999).

¹²Y. H. Ogata, R. Yasuda, T. Tsuboi, A. Otsuki, and T. Sakka, *Electrochemistry* **67**, 1203 (1999).

¹³V. Lehmann, B. Jobst, T. Muschik, A. Kux, and V. Petrova-Koch, *Jpn. J. Appl. Phys., Part 1* **30**, 2095 (1993).

¹⁴A. Bensaid, G. Patrat, M. Brunel, F. de Bergevin, and R. Herino, *Solid State Commun.* **79**, 923 (1991).

¹⁵D. Bellet, G. Dolino, and M. Ligeon, *J. Appl. Phys.* **71**, 145 (1992).

¹⁶D. Buttard, G. Dolino, C. Faivre, A. Halimaoui, F. Comin, V. Formoso, and L. Ortega, *J. Appl. Phys.* **85**, 7105 (1999).

¹⁷M. W. Cole, J. F. Harvey, R. A. Lux, D. W. Eckert, and R. Tsu, *Appl. Phys. Lett.* **60**, 2800 (1992).

¹⁸I. Berbezier and A. Halimaoui, *J. Appl. Phys.* **74**, 5421 (1993).

¹⁹Y. H. Ogata, F. Kato, T. Tsuboi, and T. Sakka, *J. Electrochem. Soc.* **145**, 2439 (1998).

²⁰Y. Ogata, H. Niki, T. Sakka, and M. Iwasaki, *J. Electrochem. Soc.* **142**, 1595 (1995).

²¹T. Tsuboi, T. Sakka, and Y. H. Ogata, *Phys. Rev. B* **58**, 13863 (1998).

²²A. R. Chelyadinsky *et al.*, *J. Electrochem. Soc.* **144**, 1463 (1997).

²³G. K. Williamson and W. Hall, *Acta Metall.* **1**, 22 (1953).

²⁴N. Nagashima and N. Kubota, *J. Vac. Sci. Technol.* **14**, 54 (1977).

²⁵M. J. Frisch *et al.*, *Gaussian 94*, Revision E.2, Gaussian, Inc., Pittsburgh PA, 1995.

²⁶W. Mönch, *Semiconductor Surfaces and Interfaces*, 2nd ed. (Springer, Berlin, 1995), p. 151.